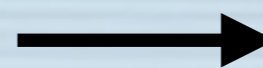


# Polarized $^3\text{He}$ targets for SBS $G_E^n$ and $A_1^n$

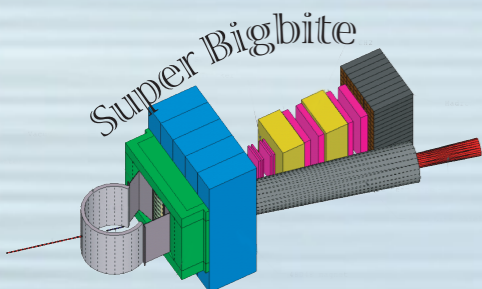
- Engineering and design on both targets
- Target-cell progress, both Stage I and Stage II
- Measurement of  $\kappa_0$  and lessons learned

Watch for this symbol to identify stuff that is  
new since last November's SBS DOE review



New since  
Nov. review

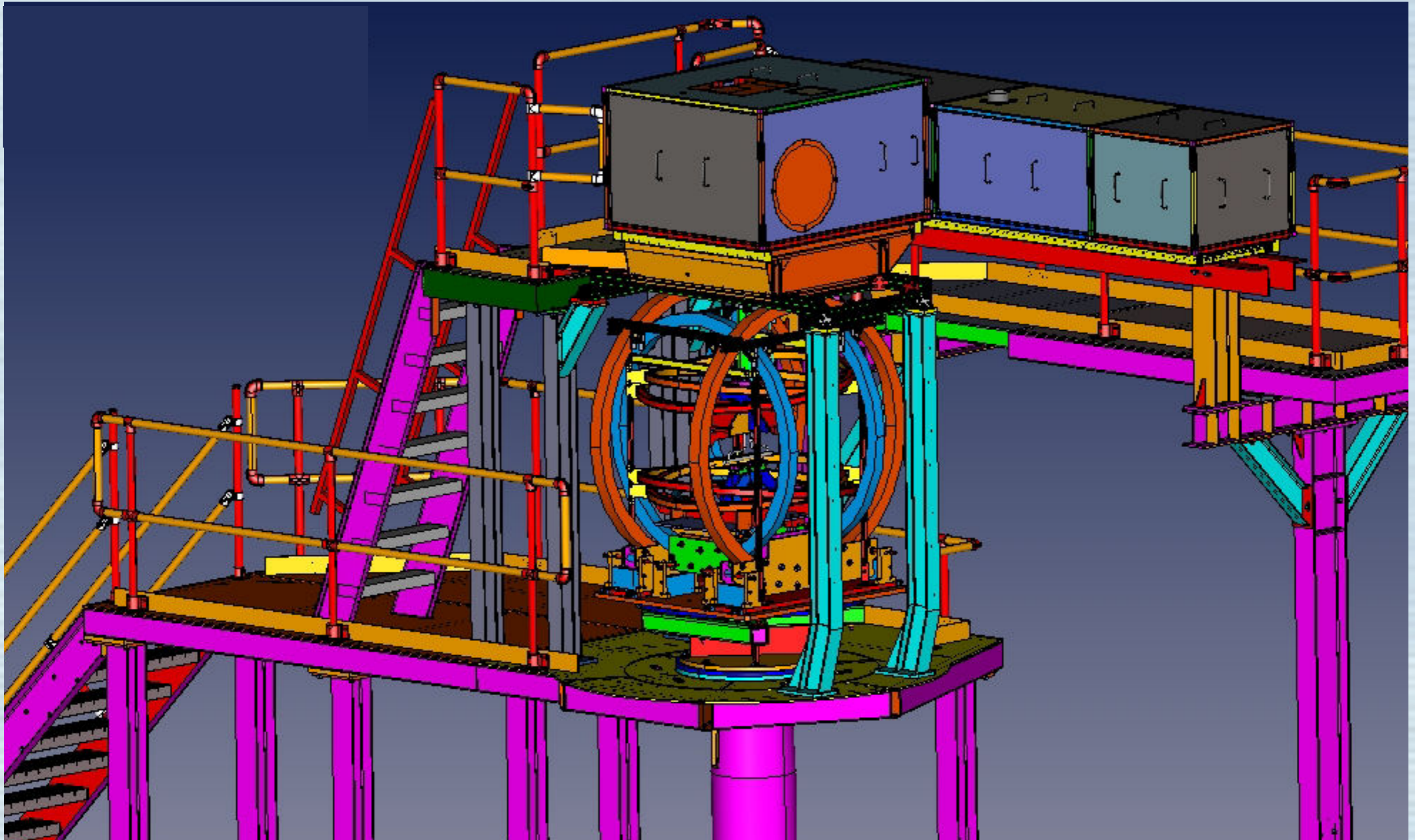
G. Cates - UVa  
July 14, 2017



# Engineering

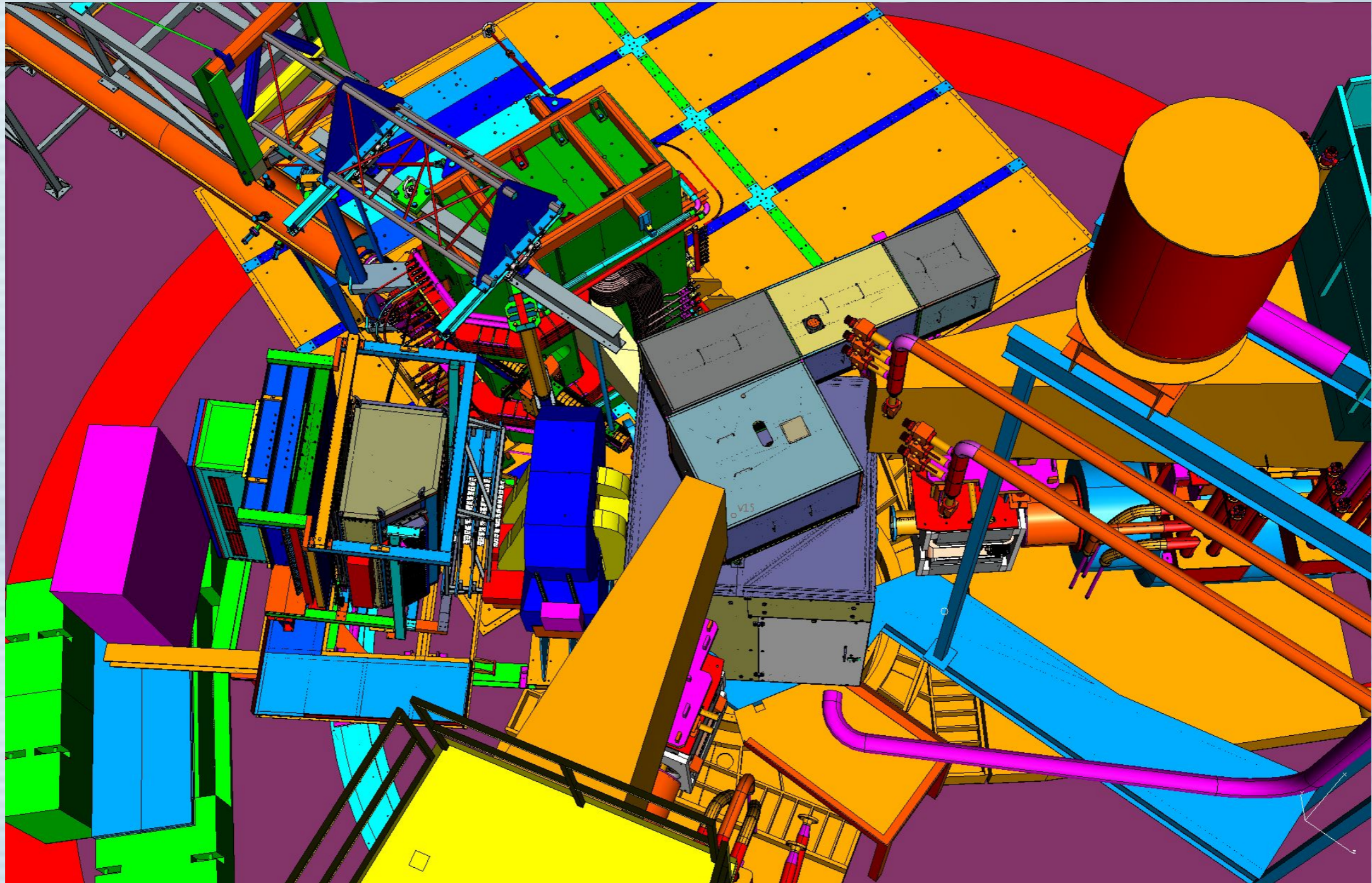


# Engineering on the Hall C $A_1^n/d_2^n$ target





# Engineering on the Hall A SBS $G_E^n$ target

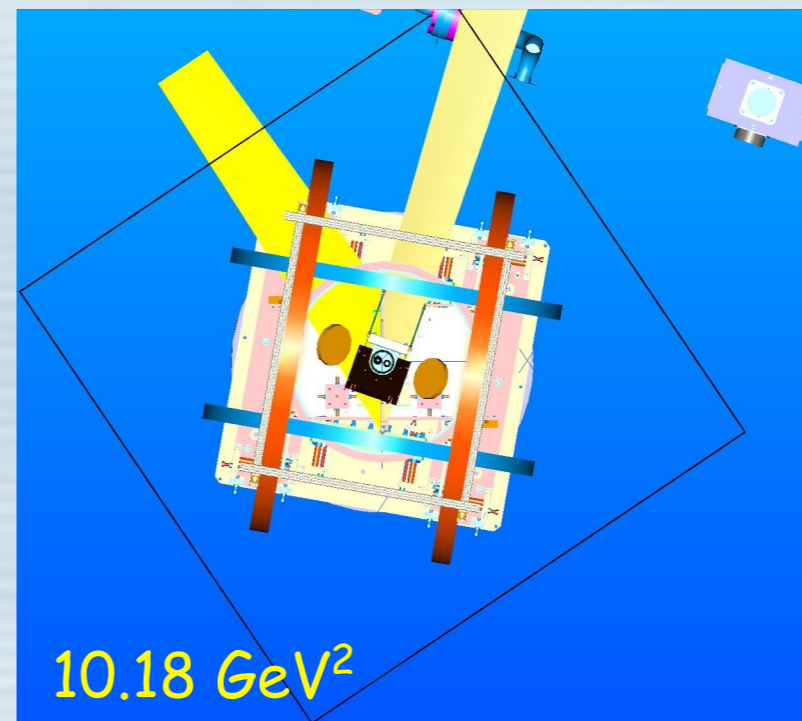
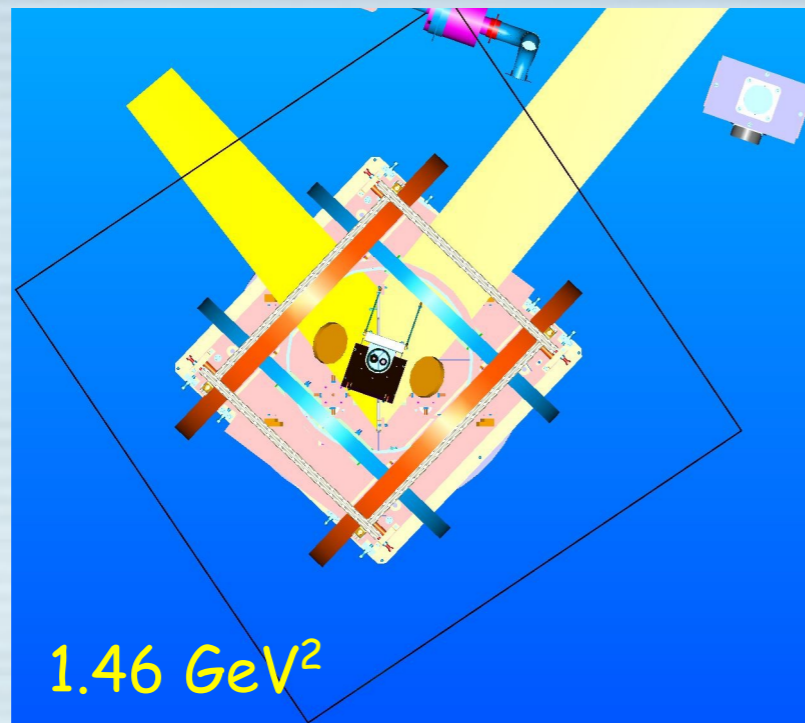


Overview of  $G_E^n$  target on the pivot.

New since  
Nov. review



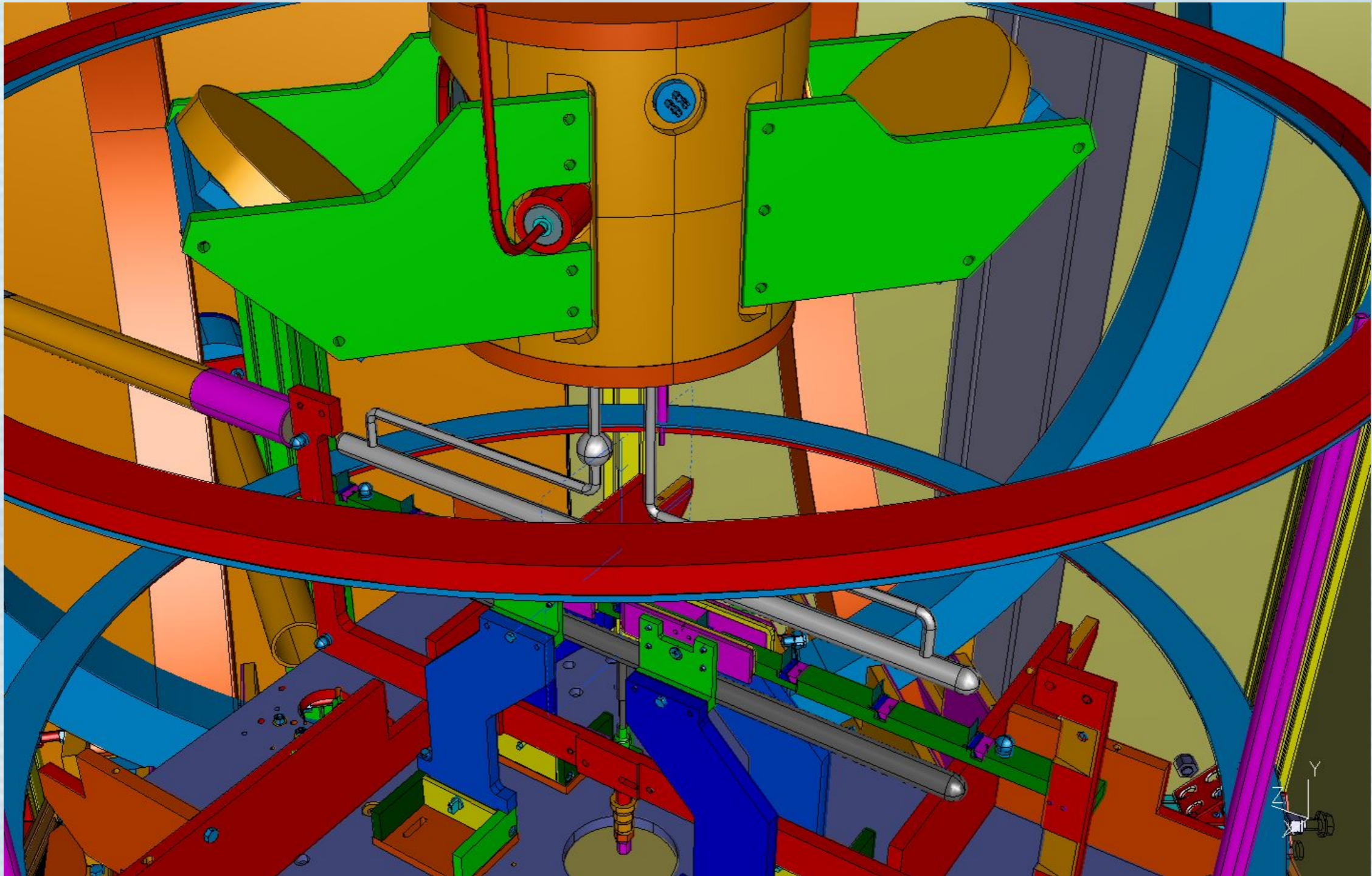
# Kinematic settings for SBS $G_E^n$ target



Design accommodates the acceptance for all kinematic points.



# SBS GEn target emphasizing target-cell region



Note TWO mirrors to bring laser light in from two directions.

New since  
Nov. review

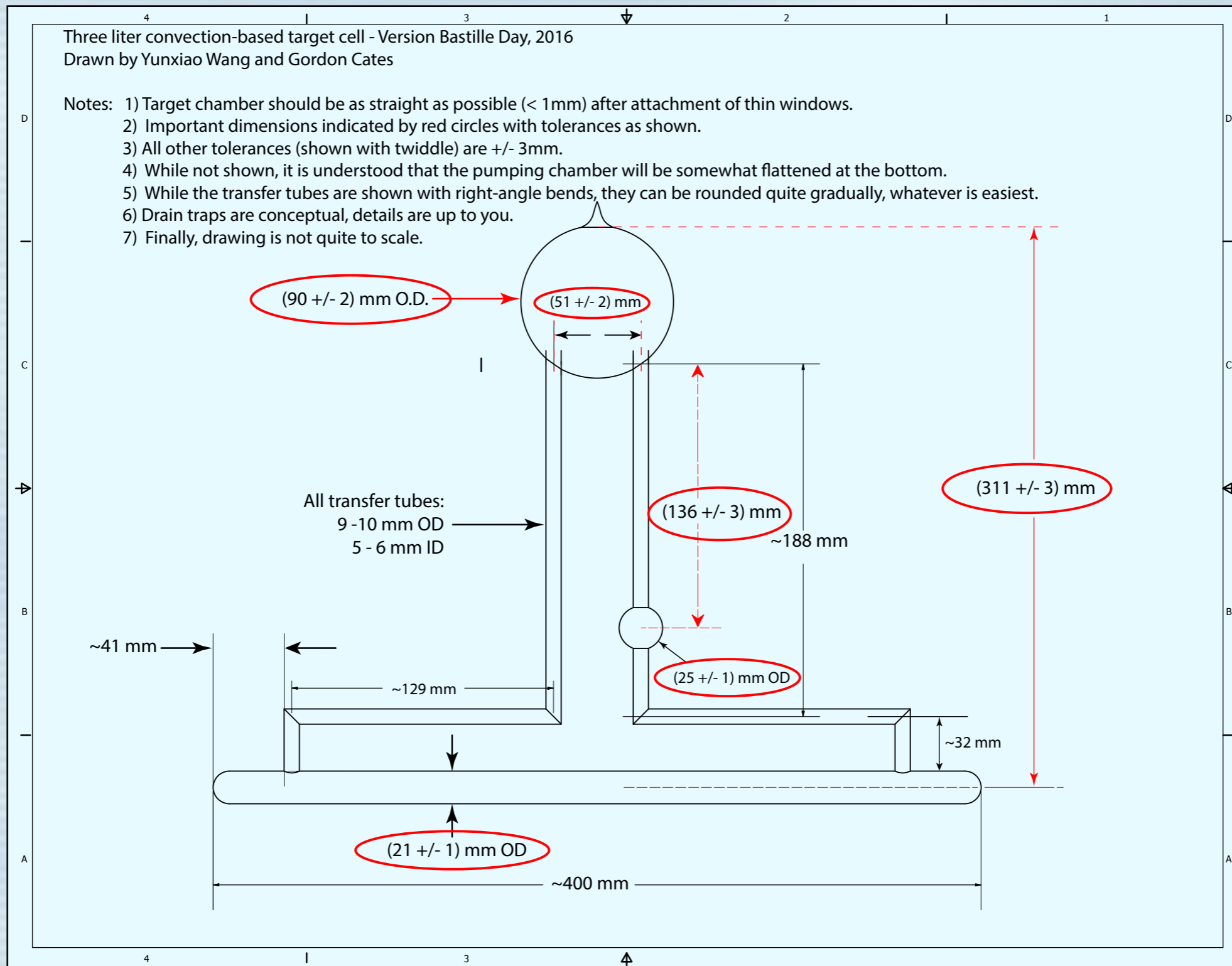


# Cell development and production

- Stage I - 3 liter cells -  $A_1^n$  and  $d_2^n$
- Stage II - 6 liter cells -  $G_E^n$  and SIDIS

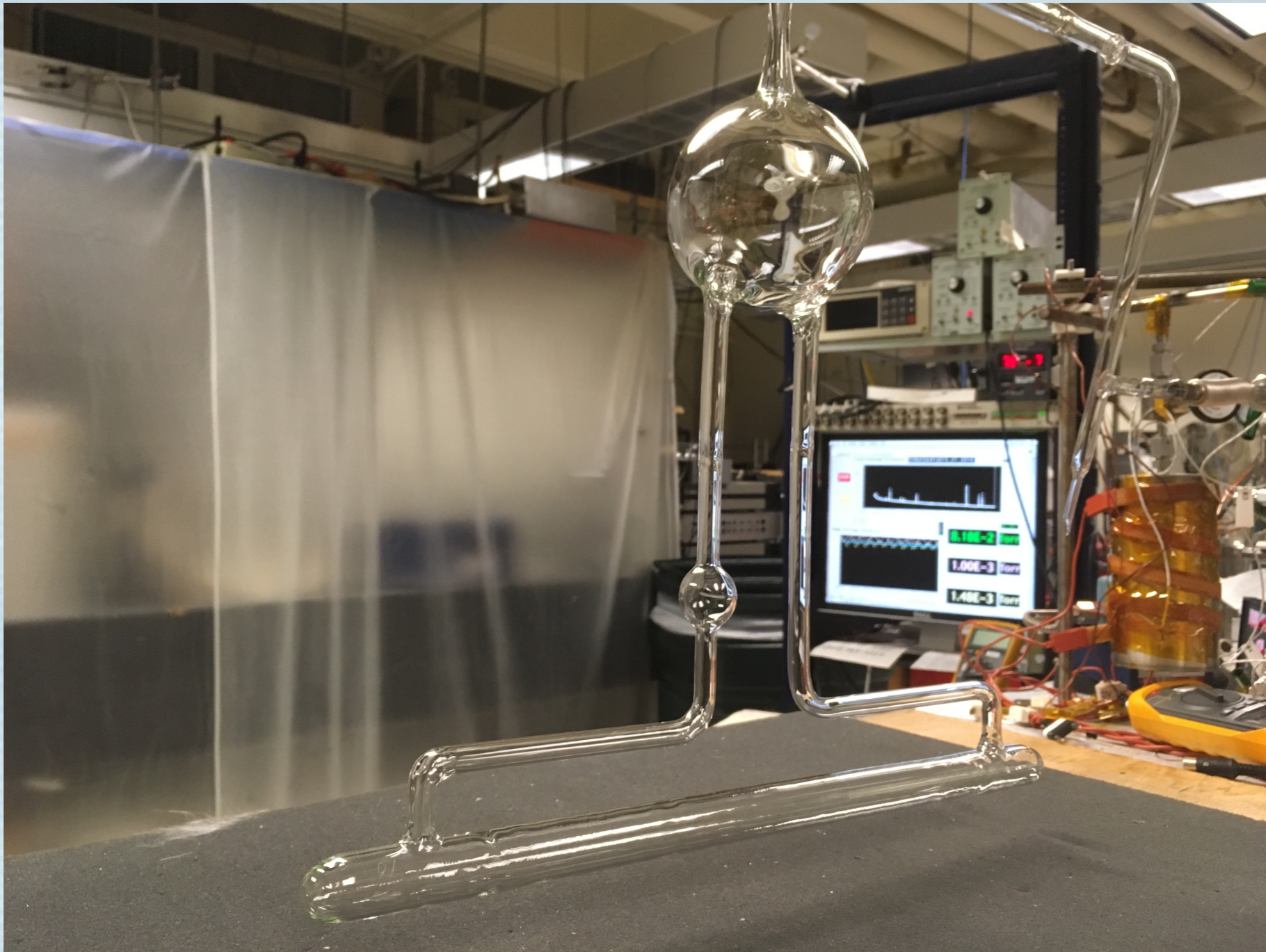


# Stage I - 3 liter - Bastille Day design (2016)





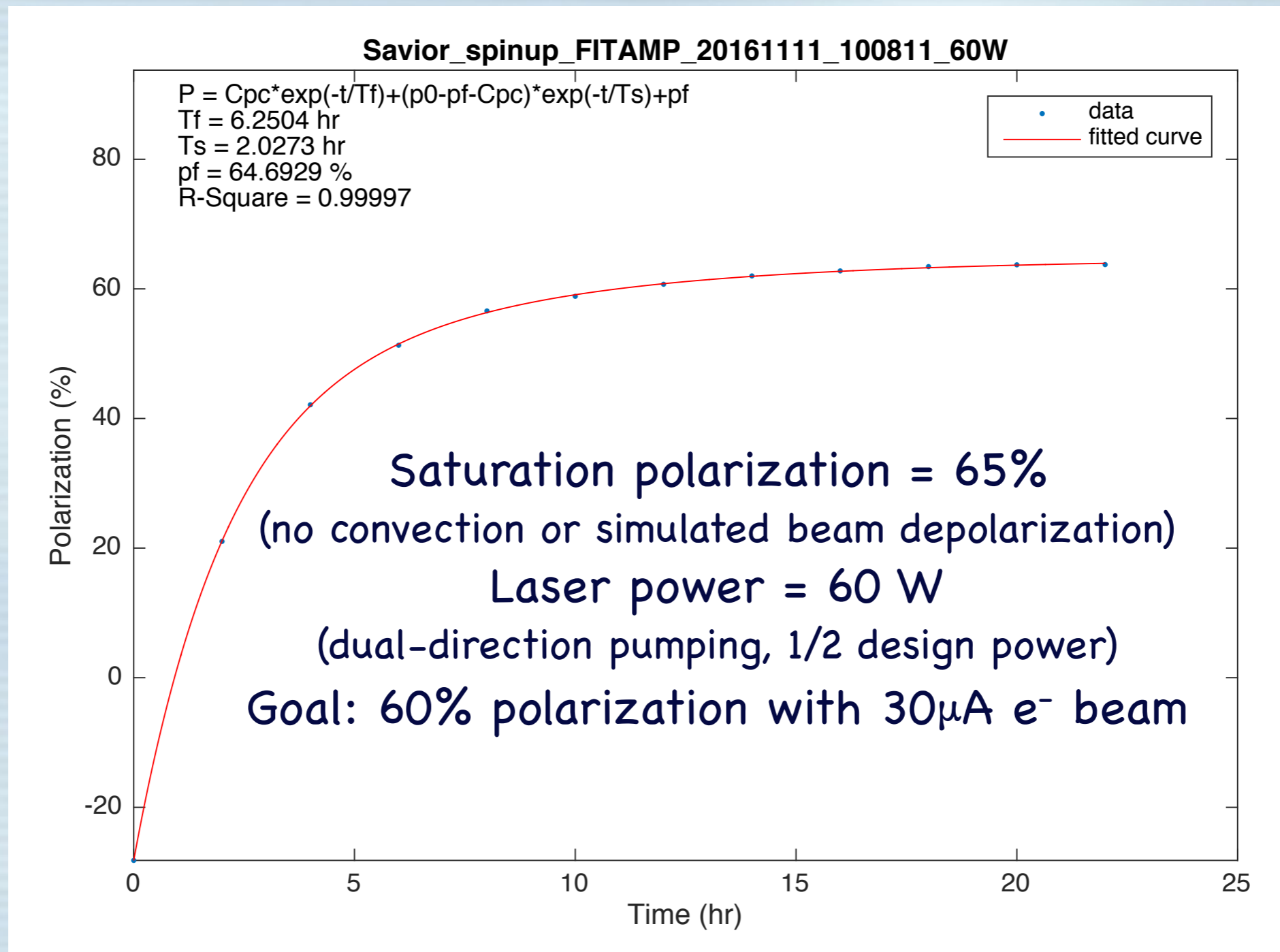
# Stage I target production underway



Shown is the Stage-I (3-liter) target cell "Savior" on the UVa gas-handling system prior to being filled.



# Stage-I polarization test of Savior

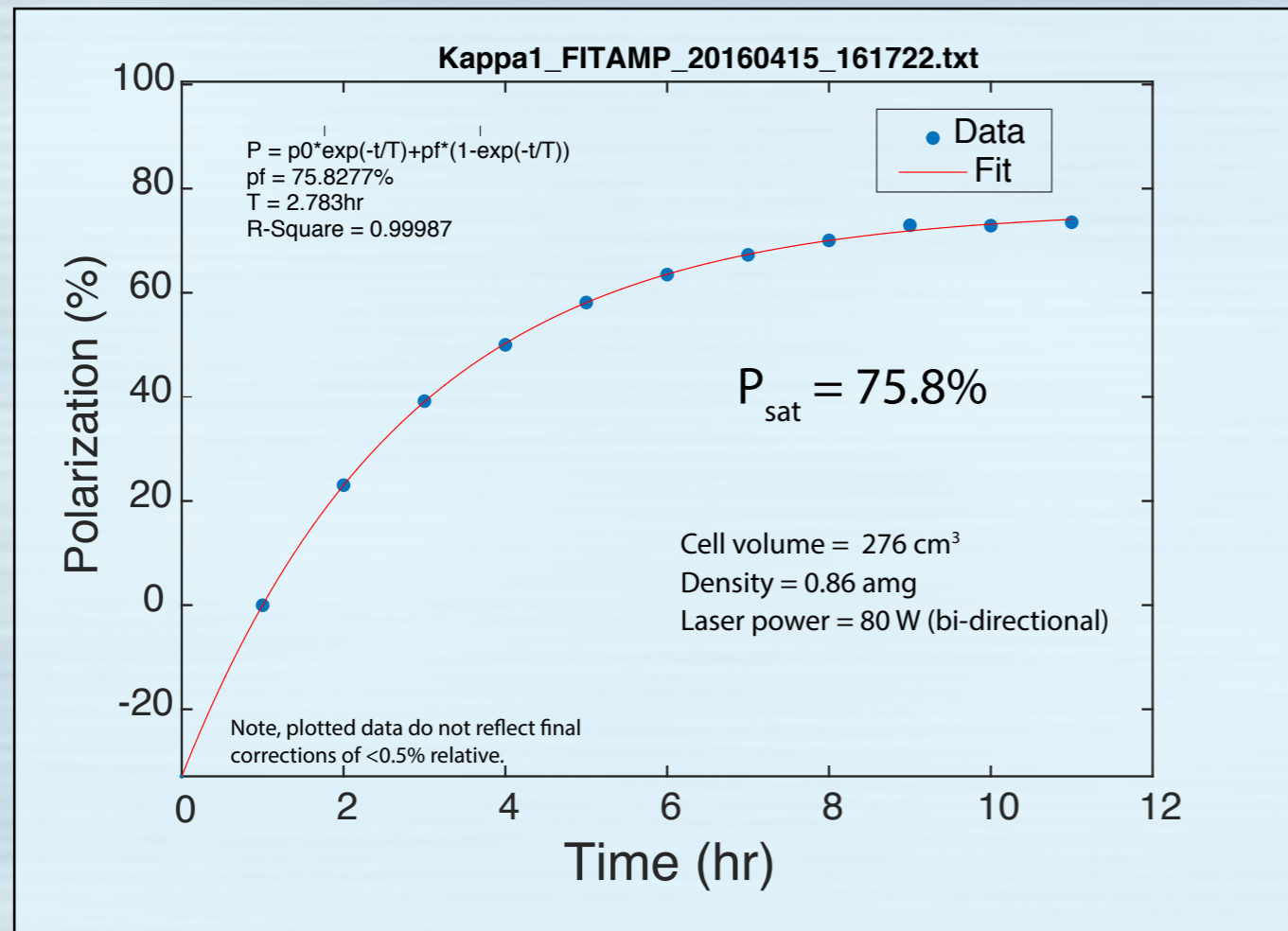


While not yet conclusive, test is very encouraging regarding the ultimate performance that is required.

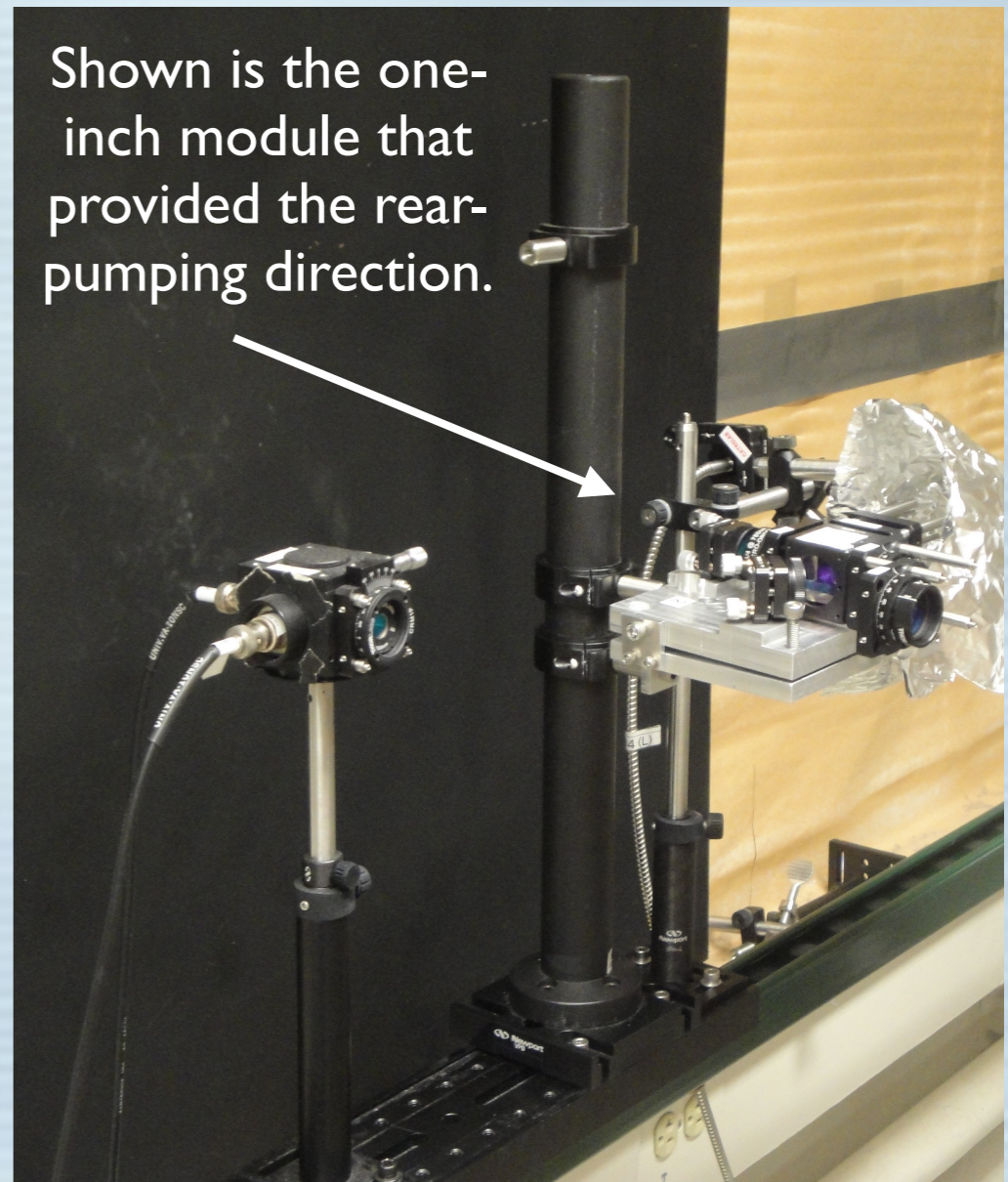
New since  
Nov. review



# First test of dual-direction pumping

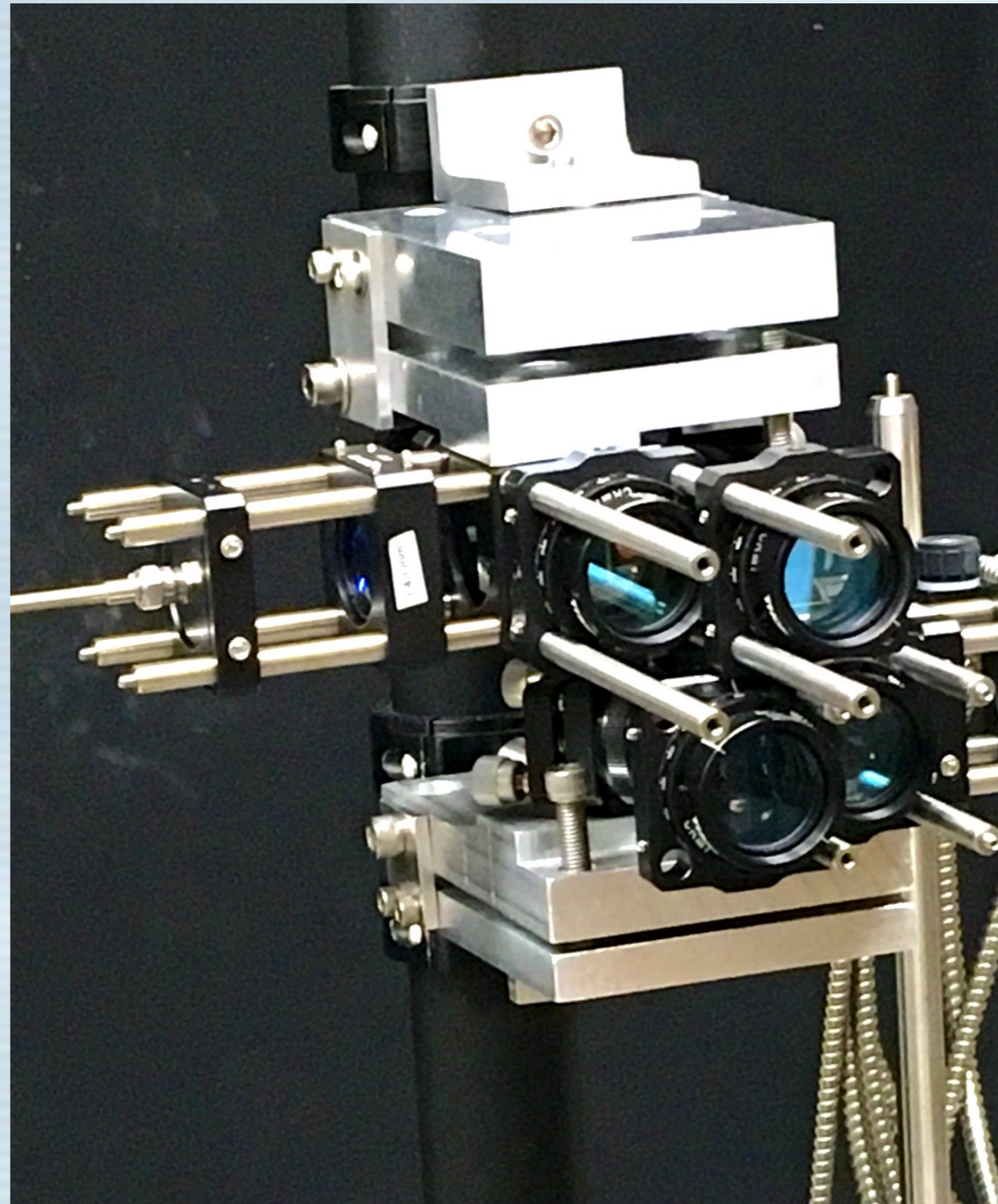


- Spherical cell, 3.25 inches outside diameter.
- Pressure just under one atmosphere.
- 40 Watts from three lasers combined with five-to-one combiner from the "front" pumping direction.
- 40 Watts from single one-inch module from the "back" pumping direction.



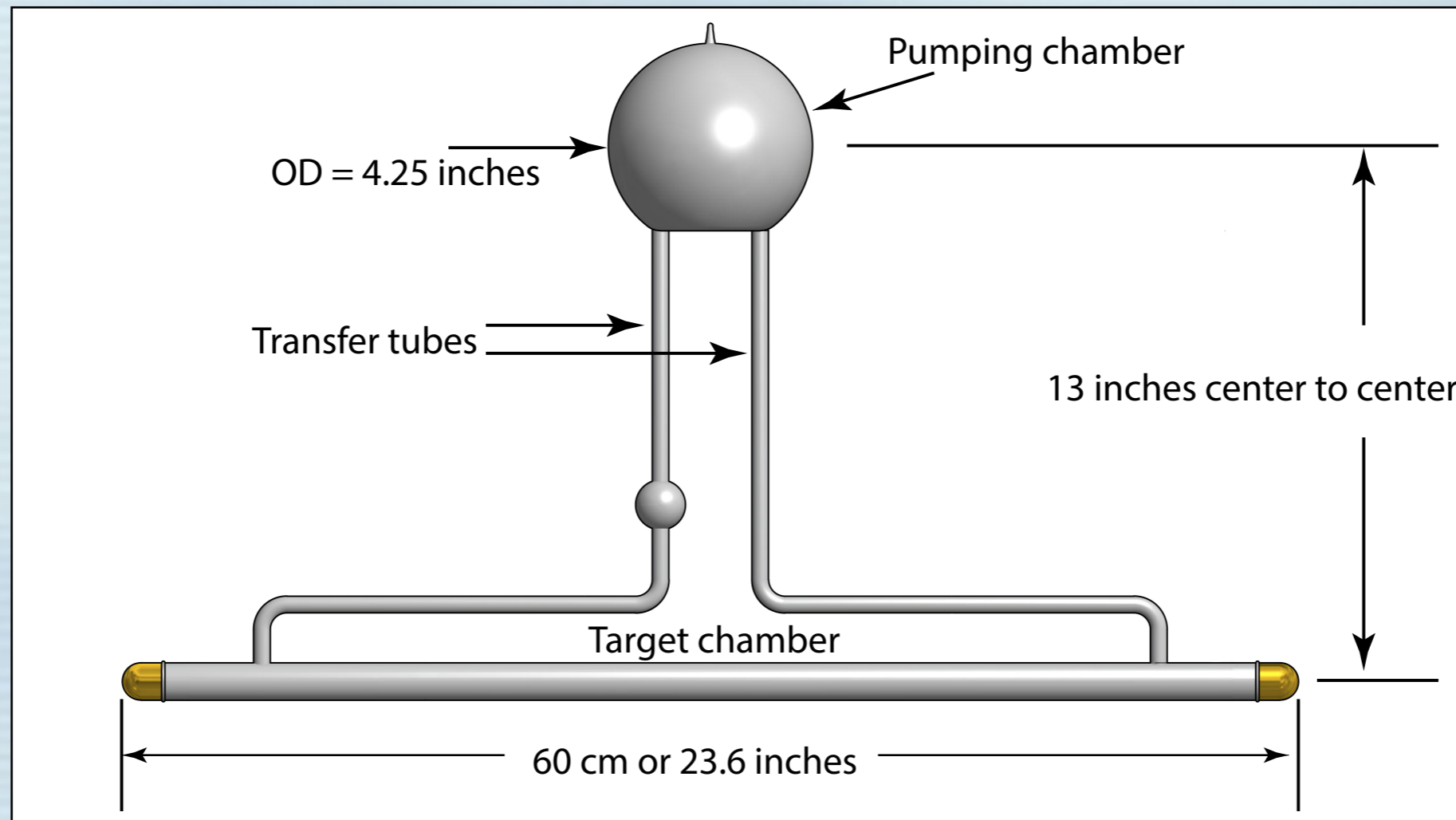


# More recent setup with two sets of optics stacked vertically





# $G_E^n$ style (Stage II) target cell design



Shown is the  $G_E^n$  target-cell design as it appears in the Target Conceptual Design Report

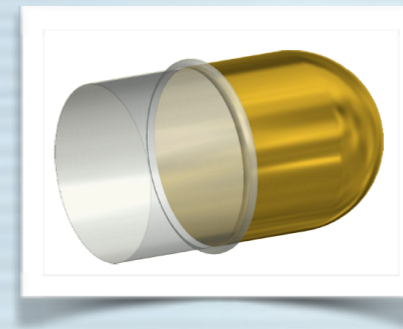
# The long road to Incorporating metal end windows

Many challenges!

- Transitioning from glass to metal with a sufficiently vacuum-tight seal that does not contaminate the gas.
  - ➔ Solved!
- Producing a metal surface, reproducibly, that does not cause excessive spin relaxation.
  - ➔ Solved!
- Identifying a material that has sufficient strength when thin enough to avoid excessive scattering that won't leak.
  - ➔ Solved, but only if the window is aluminum, which cannot be attached directly to the glass.
- If the window itself is a different piece of metal from the metal that attaches to the glass, finding a way to attach it that won't ruin bullets 1 – 3.
  - ➔ Solved (very recently) but not yet tested.



# Properties of candidate window materials



For several materials, the window thickness such that the “yield point” occurs at pressure 50% greater than the operating point. Existing GE-180 glass windows included for comparison.

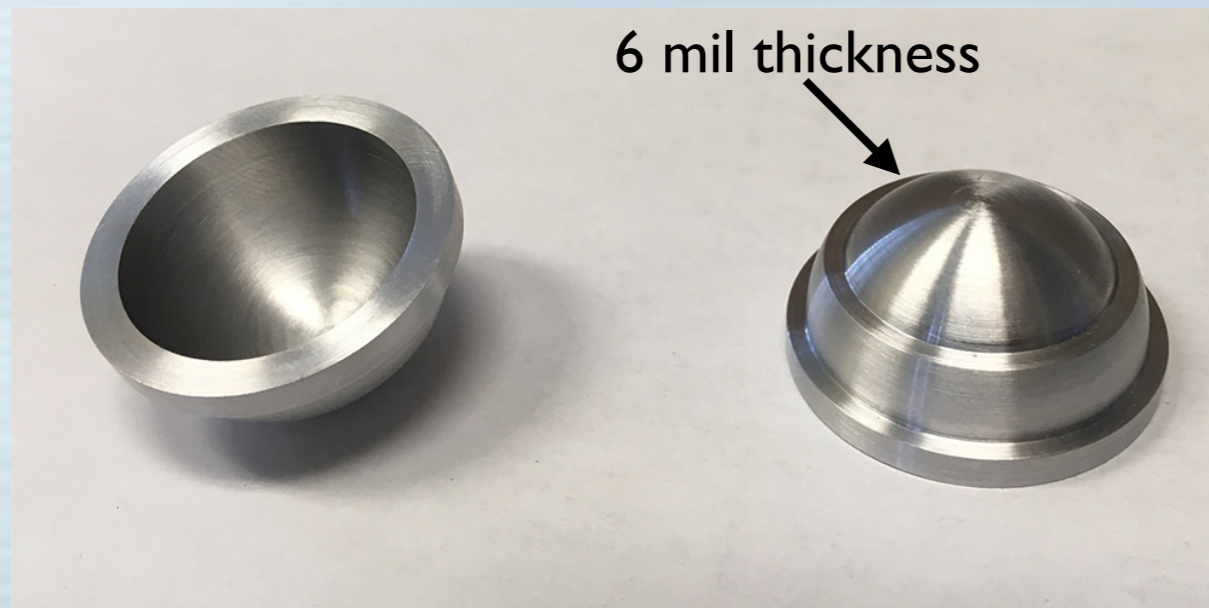
| Material        | Density (g/cm <sup>3</sup> ) | Melting Point (°C) | Yield Strength (MPa) | Min. Thickness Needed (um) | Min. Thickness Needed (mg/cm <sup>2</sup> ) | Radiation Length (mg/cm <sup>2</sup> ) | Number of radiation lengths |
|-----------------|------------------------------|--------------------|----------------------|----------------------------|---|--|-----------------------------|
| OFHC            | 8.9                          | 1065               | 49                   | 172.09                     | 153.16                                      | 1.247*10 <sup>4</sup>                  | 0.0123                      |
| Cartridge Brass | 8.53                         | 916                | 441                  | 19.12                      | 16.31                                       | 9.439*10 <sup>3</sup>                  | 0.0017                      |
| Glidcop Al-60   | 8.81                         | 1083               | 413                  | 20.42                      | 17.99                                       | 9.693*10 <sup>3</sup>                  | 0.0019                      |
| GE 180          | 2.76                         | 1015               |                      | 139.7 (thickness used)     | 38.56 (thickness used)                      | 1.388*10 <sup>4</sup>                  | 0.0028                      |
| Al              | 2.7                          | ~ 600              | 55                   | 153                        | 41.40                                       | 1.591*10 <sup>4</sup>                  | 0.0026                      |

If spin-relaxation properties are acceptable, aluminum is the preferred solution.



# Completing fabrication on first test window

The pieces shown have not yet been electroplated with gold



Region where copper will be deposited to join the two pieces



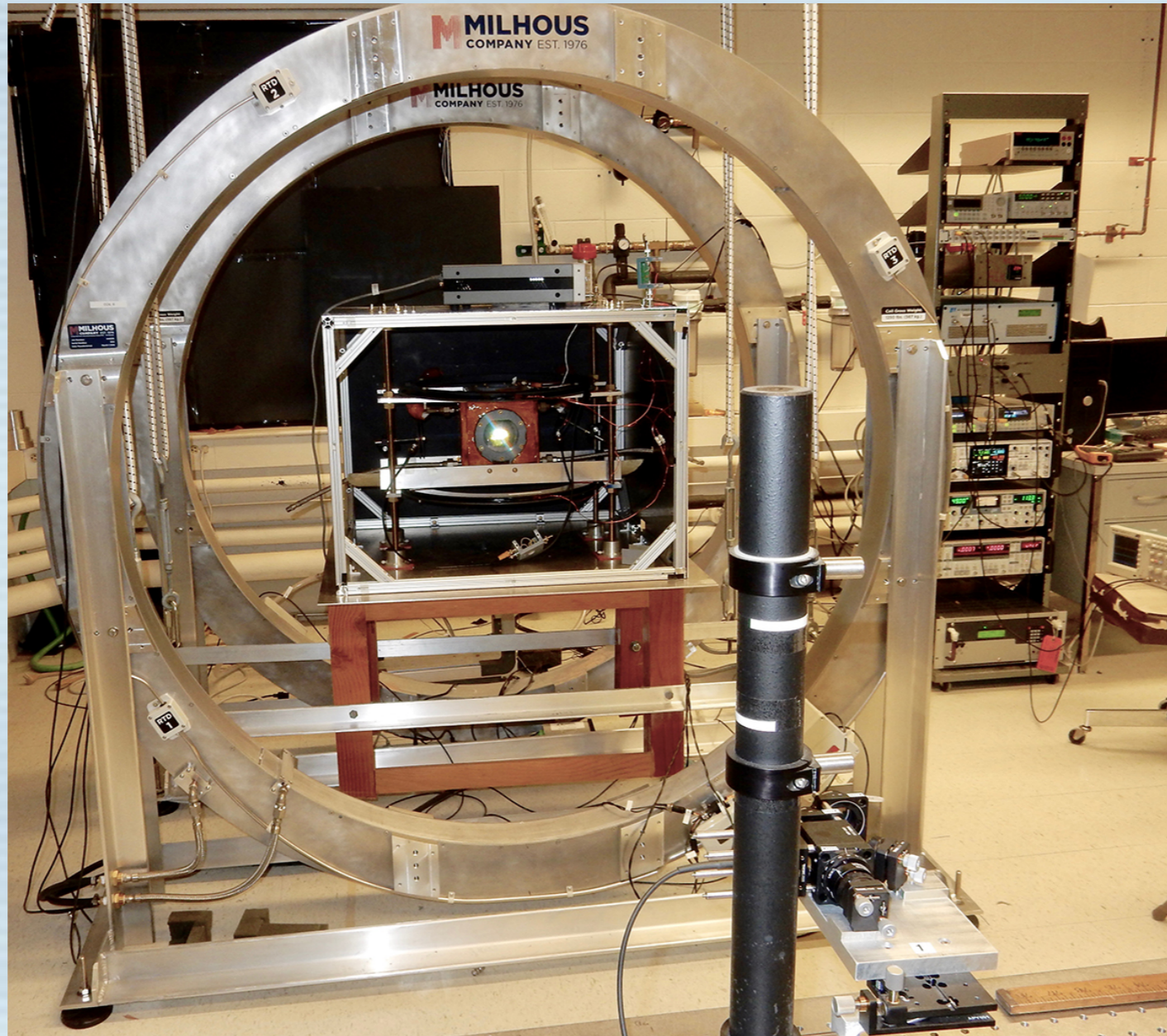
- Aluminum end-cap, machined at UVa, has 6 mil thickness with a "clear" aperture diameter of 21 mm.
- The  $^3\text{He}$  will only "see" gold surfaces.
- The end cap will be joined to the copper tube by electroplating more copper on the exterior of the point at which the two pieces meet.
- **NO HEAT IS REQUIRED FOR THE JOINING PROCESS!!!**
- The piece shown at left, once complete, will be incorporated into a test cell.



Progress on  $\kappa_0$   
measurement and  
lessons learned



# Apparatus for $K_0$ measurement

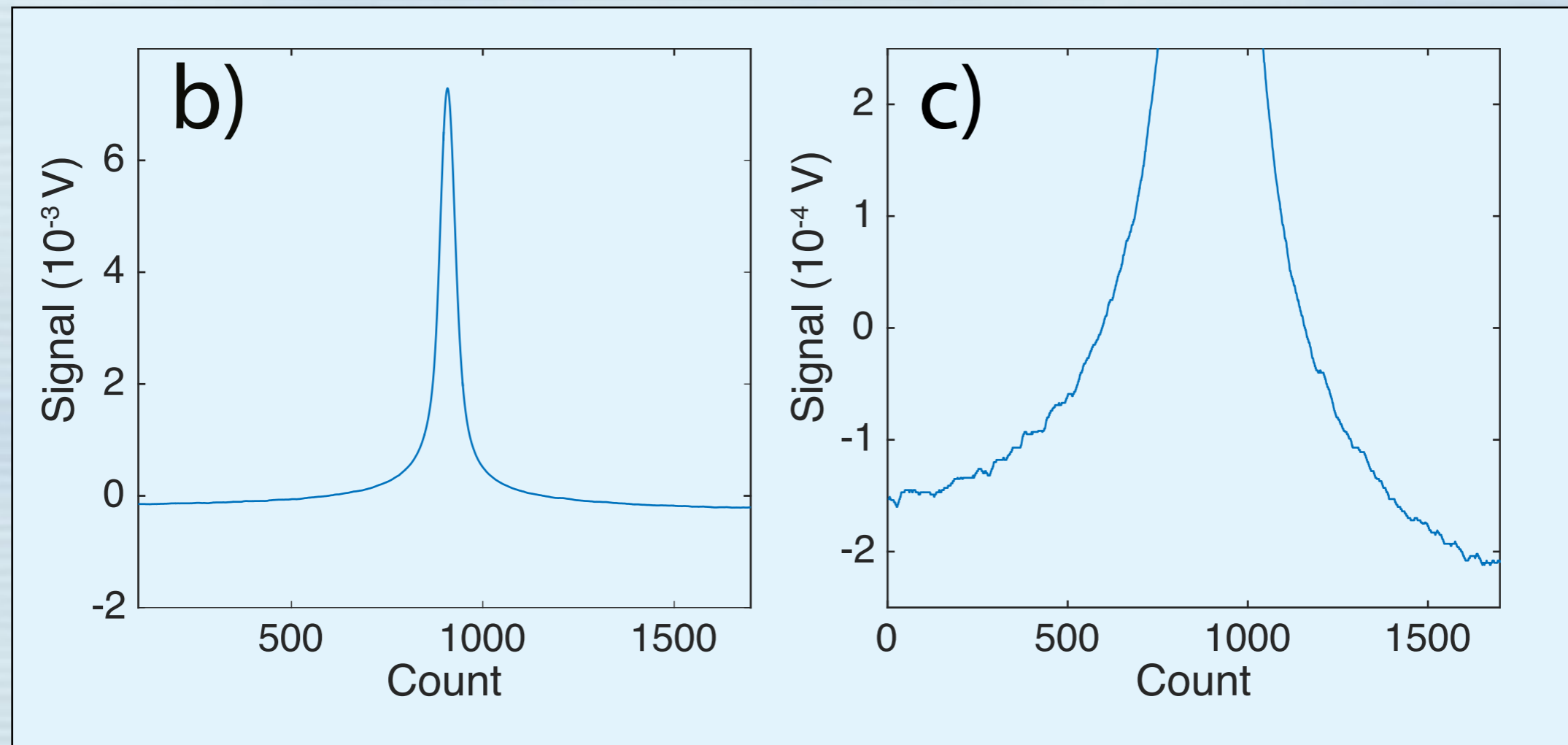


- Apparatus significantly more complete since November review
- Apparatus is suspended by bungee cords to suppress microphonic-induced noise.
- Aluminum shielding suppresses electromagnetic noise.
- Wonderful signal:noise ratio achieved.

New since  
Nov. review



# S/N ratio approaching 10000 achieved (and the system is not yet fully optimized)



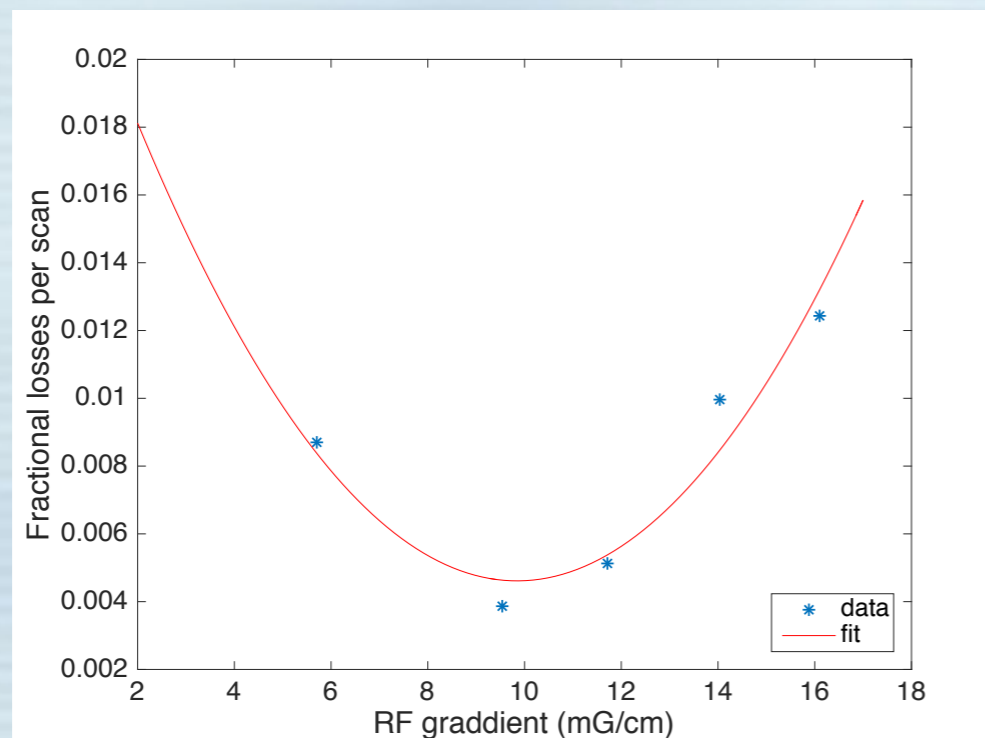
Design is working well for noise suppression.

New since  
Nov. review



# Using the $K_0$ apparatus to explore AFP issues relevant to $G_{En}$ target

We have been exploring the issues that are important for limiting AFP losses



2013 Hall A Annual Report

$$\text{fractional relaxation} = \frac{1}{T_{1\rho}} \frac{\pi B_1}{2(\partial B_z / \partial t)}$$

PRA 38, 5092 (1988) and PRL 74, 4943 (1995)

$$\frac{1}{T'_{1\rho}} = D \left[ \frac{|\nabla H_{0z}|^2}{H_{1l}^2} + \frac{|\nabla H_{1l}|^2}{H_{1l}^2} \right]$$

This term previously neglected

- Point sources of magnetic-field inhomogeneities.
- Overall inhomogeneities of the static magnetic field.
- Variations in the magnitude and direction of the RF field ( $B_1$ ).

We have identified several important effects, and are still quantifying the important issues for the  $G_{En}$  target design.

New since  
Nov. review

# Overall summary

- Engineering is on track, albeit there is much to do!
- We are formally in production of Stage-I targets (to be used in, for example,  $A_1^n$ ).
- Early polarization tests look good, again, there is much to do, but we are on track.
- The  $\kappa_0$  measurement is moving along, and has provided valuable lessons.
- There has been major progress in the metal end-window issue, although the proof will be in the upcoming tests.



**Backup slides**

# Progress and plans on target-cell production

- Stage-I target-cell production has begun.
- Oven for pressure broadening studies has been built that will accommodate the larger target cells.
- Our old Coherent 899-29 laser, used to characterize the target cells, is ailing but is probably recoverable.
- New diode-based laser is in house and we are starting the process of incorporating it into our system.
- Fast converging on metal end-window tests.
- Stage-I cell production will greatly facilitate Stage-II cell production, although there will be new challenges.



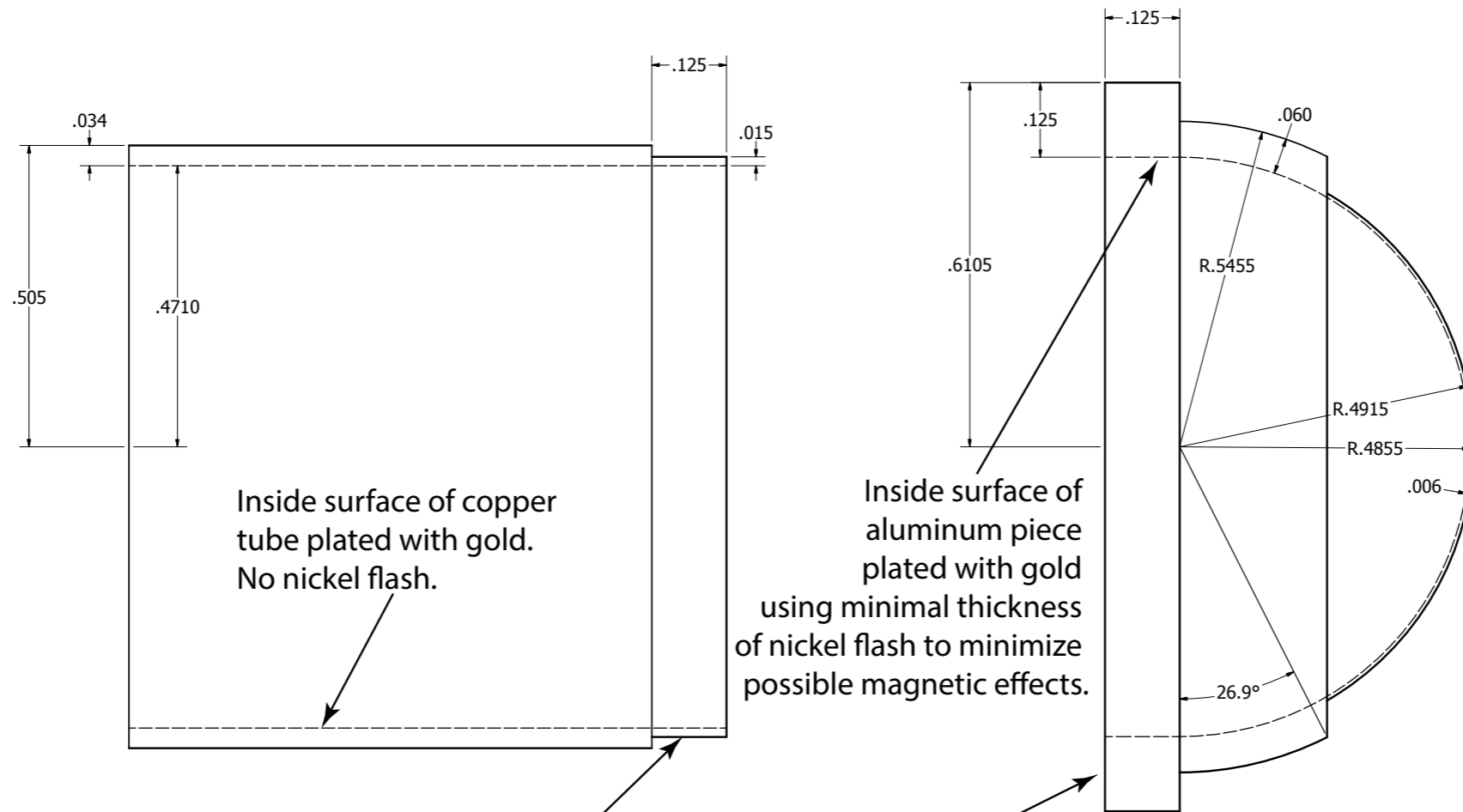
# Progress on target milestones and updates

As presented at  
November review

| *****<br>***** Target milestones *****<br>*****                   |                            |  |
|---|----------------------------|--|
| *** Selection of target cell design                               | Nov 2014                   | (Complete)                               |
| Conceptual design document complete                               | January 2016               | (Complete)                               |
| Conceptual design review  | March 2016                 | (Complete)                               |
| Start bench test of 3 liter glass conv. target                    | April 2016                 | (Complete)                               |
| Conceptual design frozen  | June 2016                  | (Complete)                               |
| Test of glass/metal technology complete                           | June 2016                  | (Complete)                               |
| Begin engineering and design                                      | July 2016                  | (Complete)                               |
| Bench test of 3 liter glass/metal target                          | January 2017 → Nov. 2017   |  |
| *** Simulated beam test (bench test)<br>(full scale 6 liter cell) | September 2017 → July 2018 |  |
| Begin production of full-scale cells                              | November 2017 → Aug. 2018  |  |
| End of engineering  | January 2018               | Cell production<br>complete<br>June 2019 |
| *** Design complete of target hardware<br>and Instrumentation     | June 2018                  |  |
| *** Target is ready   | January 2019               |  |
| *****<br>*****<br>*****   |                            |  |

Mtg. this afternoon to determine  
Probably March 2019?

# Details on electroplating



Inside surface of copper tube plated with gold. No nickel flash.

Inside surface of aluminum piece plated with gold using minimal thickness of nickel flash to minimize possible magnetic effects.

Outside surface of copper tube in region that mates with aluminum piece plated with gold. No nickel flash.

Exterior of aluminum "flange" facing the copper tube plated with copper in preparation for joining

|          |  |   |        |              |
|----------|--|---|--------|--------------|
| DRAWN    |  | Drawing by Chris Jantzi and Gordon Cates<br>July 12, 2017 |        |              |
| CHECKED  |  | TITLE   |        |              |
| QA       |  | UVa glass-to-copper and aluminum endcap assembly          |        |              |
| MFG      |  | SIZE  | DWG NO | REV          |
| APPROVED |  | C   |        |              |
|          |  | SCALE   | 8 : 1  | SHEET 1 OF 1 |



# Relaxation due to inhomogeneous magnetic fields during resonance conditions

This paper, the usual reference for AFP losses, neglects the effects of inhomogeneous RF fields.

PHYSICAL REVIEW A

VOLUME 38, NUMBER 10

NOVEMBER 15, 1988

## Spin relaxation in gases due to inhomogeneous static and oscillating magnetic fields

G. D. Cates, D. J. White, Ting-Ray Chien, S. R. Schaefer, and W. Happer  
*Department of Physics, Princeton University, Princeton, New Jersey 08544*  
 (Received 27 June 1988)

We have extended a recent theory of spin relaxation in gases due to static magnetic field inhomogeneities to include the effects of oscillating magnetic fields. We use this theory to show how magnetic field inhomogeneities cause spin relaxation under magnetic resonance conditions. We have confirmed some of the main theoretical predictions by experimental observations. Spin relaxation in inhomogeneous magnetic fields can be used as a convenient new way to measure diffusion constants in gases.

Recent studies of the effects for earlier target work at JLab seemed to describe things nicely.

$$\frac{1}{T_{1\rho}} = \frac{|\vec{\nabla} B_z|^2}{B_1^2} D$$

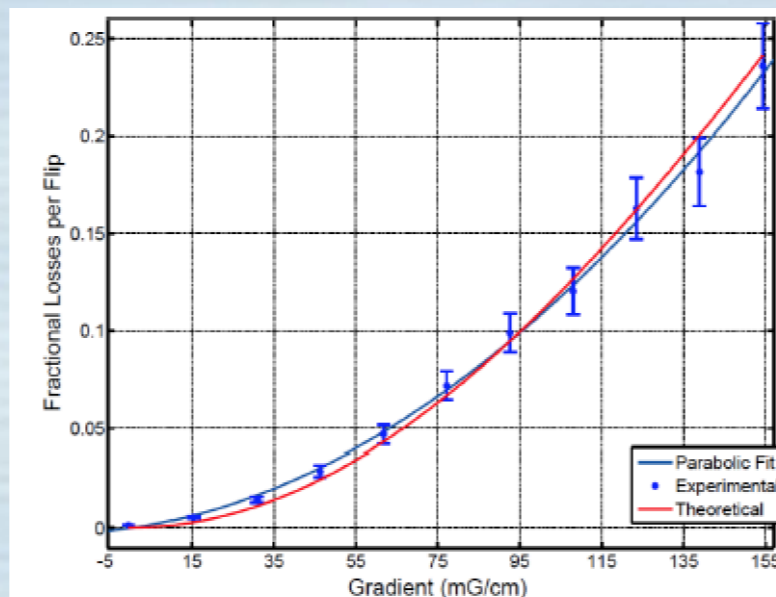


Figure 3.4: Fractional AFP loss (single flip) as a function of field gradient.

However, a later paper by Driehuys, Cates and Happer considered conditions where the RF inhomogeneities needed to be included:

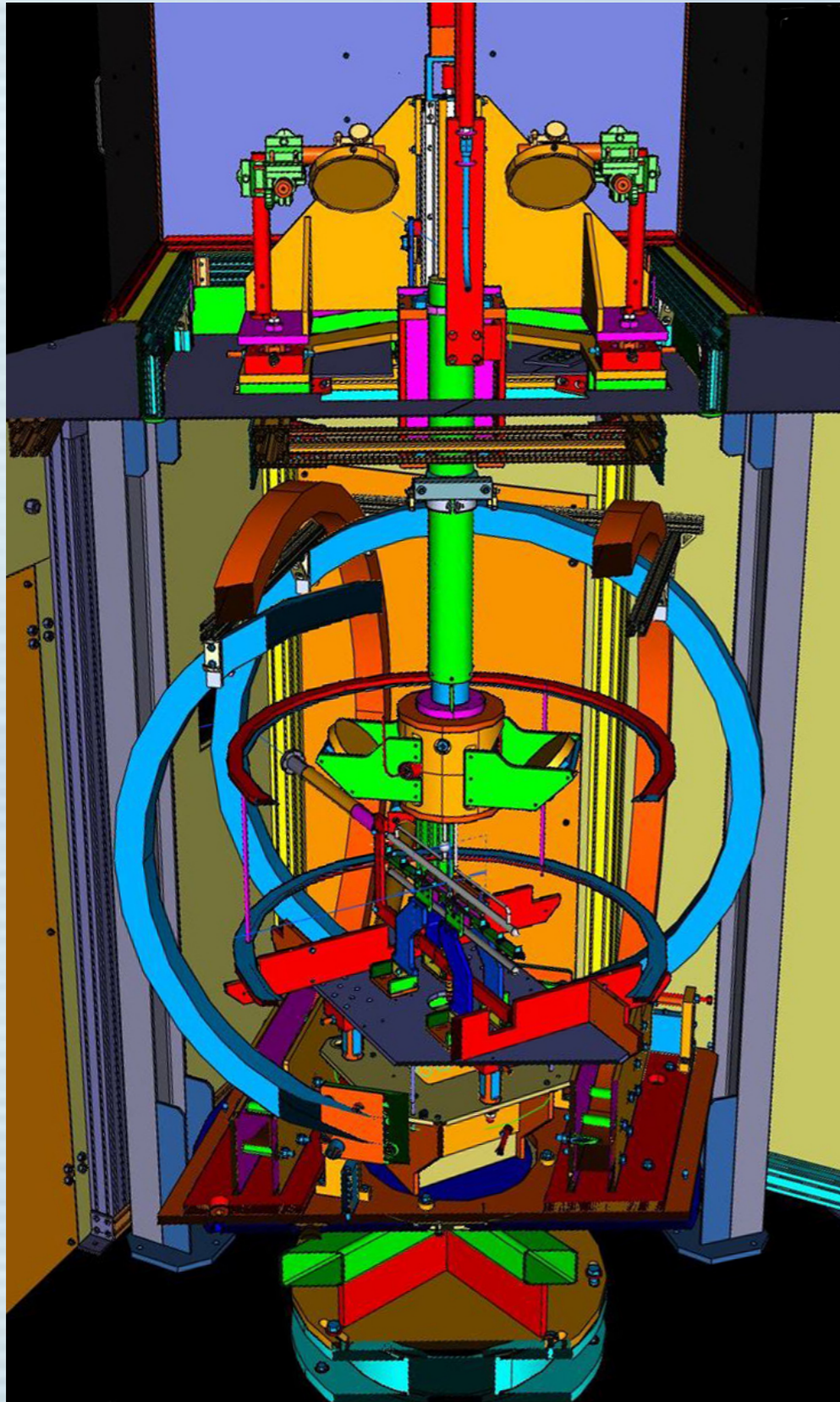
PRL 74, 4943 (1995)

$$\frac{1}{T'_{1\rho}} = D \left[ \frac{|\nabla H_{0z}|^2}{H_{1I}^2} + \frac{|\nabla H_{1I}|^2}{H_{1I}^2} \right]$$

New since  
Nov. review



# Current state of the engineering design

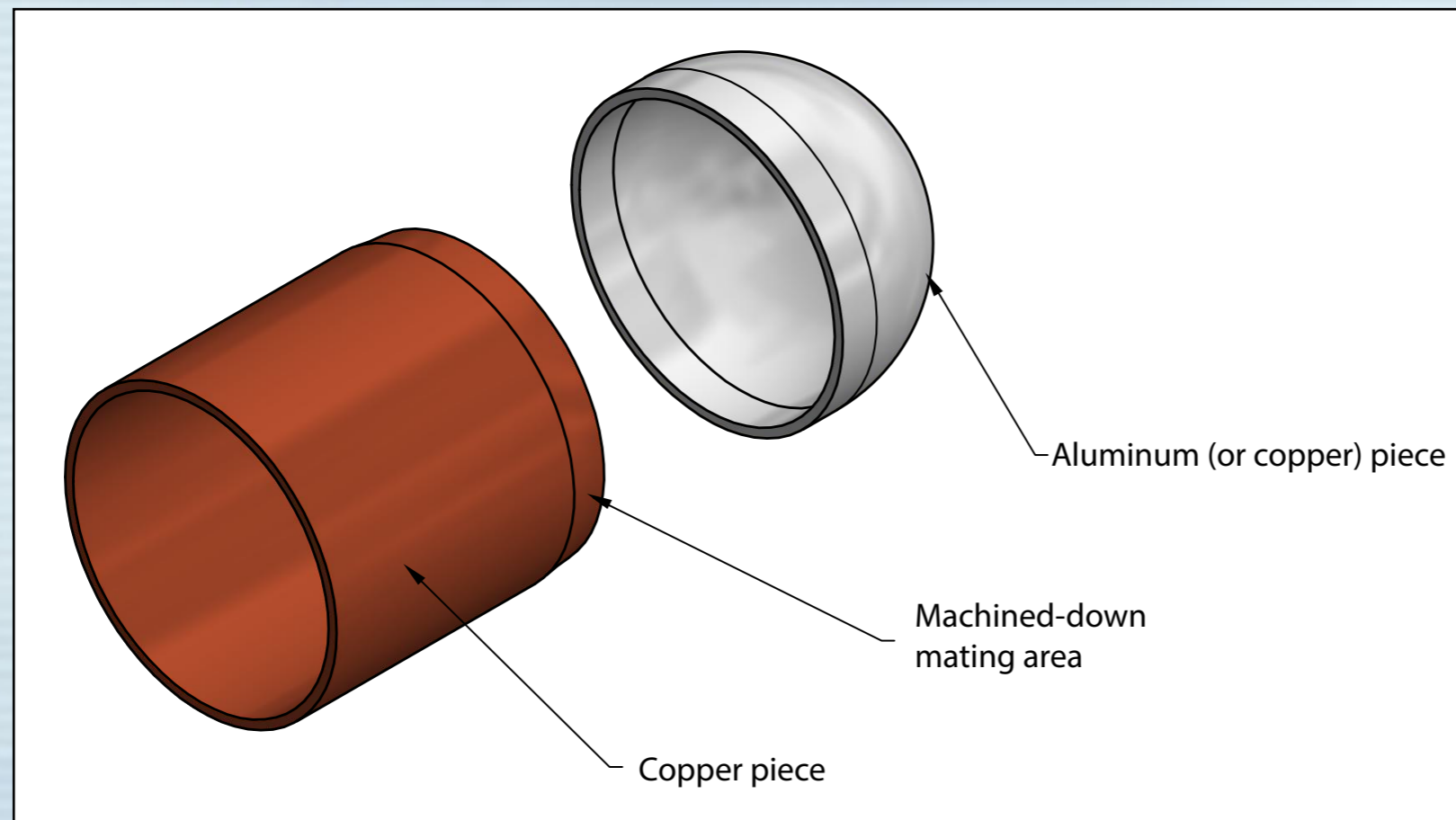


Closeup emphasizing target ladder.

New since  
Nov. review



# Thin window development



- Aluminum is an attractive material for the end windows, but gold-coated aluminum has not yet been tested for its spin-relaxation properties.
- We are in conversation with Epner about the best way to attach and coat the aluminum "end cap".
- Hope to construct and study test cells with aluminum end caps within one or two months.
- A successful test could lead to a target cell with metal end windows within one to two months after successful test (3-4 months out).





